ISSN : 0974 - 7540 Volume 5 Issue 6

Research & Reviews On Electrochemistry

Full Paper

RREC, 5(6), 2014 [155-168]

A neural network model for quantitative prediction of oxide scale in water walls of an operating Indian coal fired boiler

Amrita Kumari[1]*, S.K.Das[2], P.K.Srivastava[1]

[1]Birla Institute of Technology, Ranchi 835 215, (INDIA)

[2]CSIR-National Metallurgical Laboratory, Jamshedpur 831 007, (INDIA)

E-mail: amrita_pandey@dvcindia.org

ABSTRACT

Application of artificial neural network (ANN) for predicting industrial process behavior has been increasingly popular in the power sector industry. In this paper, a multi-layer perceptron (MLP) based ANN model has been developed to predict the deposition rate of oxide scale on waterwall tubes of a coal fired boiler. The input parameters in the ANN model are boiler water chemistry and relevant operating parameters, namely, pH, alkalinity, total dissolved solids, specific conductivity, iron and dissolved oxygen concentration of the feed water and heat flux of a typical 250 MW coal fired boiler. The neural network architecture has been optimized using an efficient gradient based network optimization algorithm to minimize the training and testing errors rapidly during simulation runs. The parametric sensitivity of heat flux, iron content, pH and the concentrations of total dissolved solids in feed water and other operating variables on the scale deposition behavior has also been investigated. It has been observed that heat flux, iron content and pH of the feed water have a relatively predominant influence on the oxide scale deposition phenomenon. There has been very good agreement between ANN model predictions and the measured values of oxide scale deposition rate substantiated by the regression fit between these values.

© 2014 Trade Science Inc. - INDIA

KEYWORDS

Boiler corrosion;
ANN model;
Oxide deposition;
Water chemistry;
pH;
Heat flux.

INTRODUCTION

Corrosion and Scaling are the major waterside problems in industrial boilers. Various compounds of calcium, magnesium, iron, copper and silica are predominant elements found in most of the boiler scales. These scales usually form a dense layer that impedes heat transfer and cause boiler tube failures leading to outages. Most corrosion products that deposit as oxide scales in the boiler originate in the pre-boiler (up-stream) systems. The majority of the boiler scales consist of colloidal and particulate metals and their oxides. The compounds are swept into the boiler and deposit on boiler tube surfaces primarily as oxide scales. Corrosion not only contributes to scale deposition, but also eventually leads to materials damage.

Full Paper

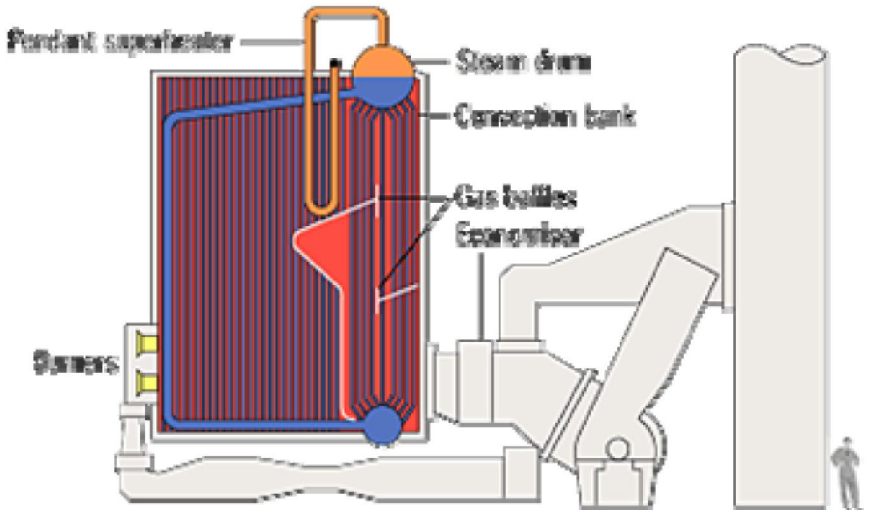

Figure 1 : Schematic of water-tube boiler assembly

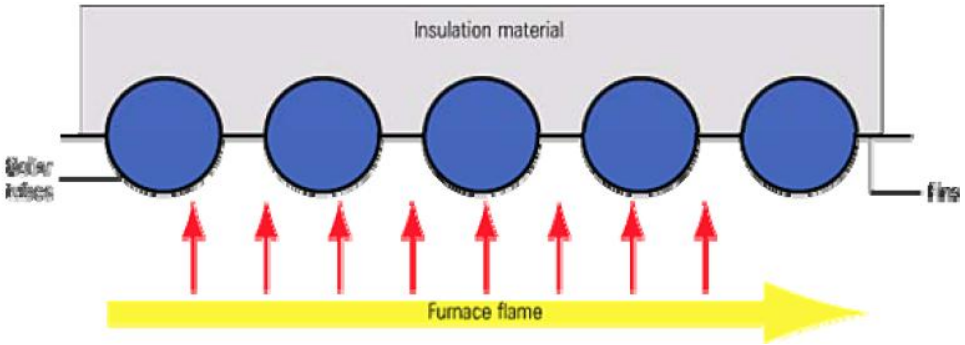

Figure 2 (a) : Heat transfer in the radiant section

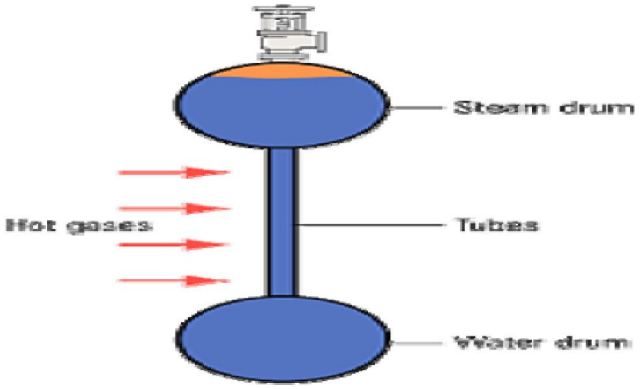

Figure 2 (b) : Heat transfer in the convection section

Reliability of operation of heat transfer surfaces of coal fired boilers is determined mostly by deposition rate on these surfaces such as boiler water walls, superheater and reheater. Figure 1 shows a simplified schematic of a coal fired sub critical boiler. Numerous laboratory and field test results have shown that oxide scales are deposited non-uniformly along the height of boiler waterwalls and others associated components[1,2]. The predominant amount of scales gets deposited in high heat flux zones in the boiler assembly. In spite of more rigid requirements towards feed water purity, the deposition rate on heat exchanging surfaces in boilers has been increased due to higher operational requirements. Once there is a scale builds-up on a heat transfer surface, at least two associated problems do occur. The first problem is the degradation in the performance of heat transfer equipment. The second less critical problem is that a small change in tube diameter substantially decreases the flow rate or increases the pressure drop in the heat transfer equipment. This results in decrease in operational period between cleanings and increases the risk of equipment failures. Figure 2[a] and [b] show the schematics of heat transfer modes in the radiant and convective section of coal fired boiler. Corrosion and scale deposition are time-dependent phenomenon. Nevertheless, the widely used method for designing industrial boilers and heat exchangers exposed to a corrosive environment is to use empirical methods for corrosion resistance associated with scale formation. In general, empirical methods based on classical sta-

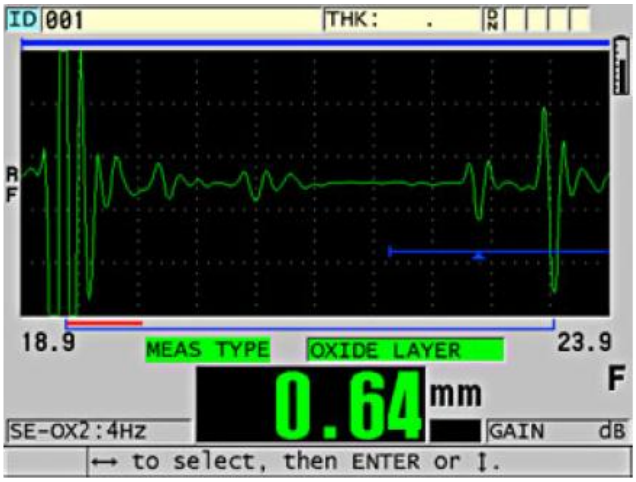

(a)

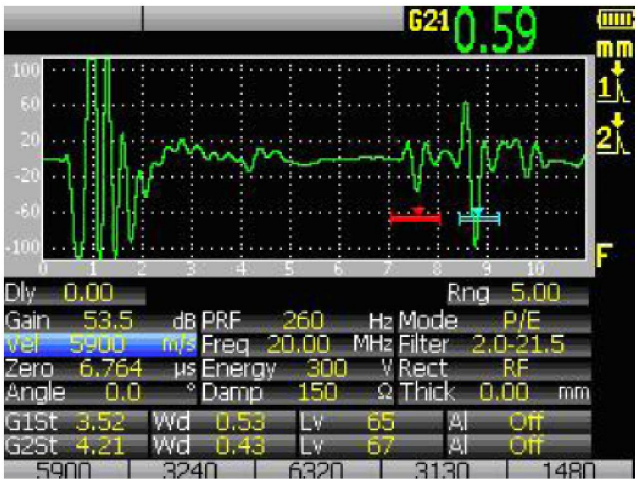

(b)

Figure 3(a) & (b) : Typical view of the signal wave forms during oxide scale measurement

tistical technique are not capable of estimating quantitatively the quantum of scale deposition and corrosion loss with reasonable degree of accuracy. Thus, it may be probable that the equipment will have to be taken out of service for cleaning at an inconvenient and economically undesirable time. In order to provide an estimate of operational longevity of boiler tubes for a desirable period of operation, it is necessary to be able to predict the scale deposition and corrosion behavior as function of both time and operational parameters[3-5].

Due to increased feed water (Recycled condensate and makeup *water*) purity in coal fired both subcritical and supercritical boilers, the scales form on steam generating surfaces mostly consist of corrosion products of construction materials, i.e. iron and copper oxides. Since forms of existence of iron and copper corrosion products (scales) depend on water chemistry, the deposition rate of the above mentioned impurities would depend on the nature of chemical water treatment. The major constituent of the oxide scale is iron oxide. Therefore, optimization of water chemistry is an important operational issue, in particular for the power plants with mixed metallurgy. The most popular water treatment scheme for sub-critical boilers is ammonia/ hydrazine feed water treatment, also known as all volatile treatment (AVT). When the tube metal is in contact with the steam over period of time, the oxidation process may begin to form a layer of magnetite (Fe_3O_4) scale. In the prolonged exposure this phenomenon will worsen situation that leads to potential creep rupture problems. Scales inside the superheater and reheater steam tubes have also been found to be one of the major contributors to the tube failure. Heat transfer rate across the tube also decreases due to the accumulated scales inside the tube. A further effect of growing scales is that the tube will operate at relatively higher temperatures than those as originally specified. Such exposure may cause degradation of the tube alloy, and this eventually will lead to tube rupture. It is estimated that 10% of all power-plant breakdowns are caused by creep fractures of boiler tubes due to the scales formation[2].

Chemistry of deposition of oxidation-corrosion products

Concentration of iron corrosion products in boiler water, in general, exceeds iron solubility. These products may have different sizes and carry electrical charges. In this case, deposition mechanism may be explained by particle charge due to both ion adsorption ability from water and transport of hydroxyl-ions from particle surface layer to water[2]. Polarity and magnitude of iron corrosion particle charge is given by both molecular and fluid properties with predominant influence of potential forming ions, among other factors. Water chemistry with no additions of conditioning chemicals, these potential-forming ions for iron oxides are either OH- or H+. Therefore, iron corrosion products deposition rate kinetics depends critically on fluid pH. The scales, in general, comprise of Hematite (Fe_2O_3), Magnetite (Fe_3O_4), Quartz (SiO_2), Wallastonite ($CaSiO_3$), Calcite ($CaCO_3$) and Brucite ($MgOH_2$) etc.

Boiler water is normally maintained in an alkaline range (pH of 9 - 11 depending upon the boiler type and

pressure) to prevent acidic attack. This pH range is moderately basic and small amounts of caustic alkalinity (OH-) may be present in the bulk of boiler water. The boiler water side tube walls develop a tightly bound layer of magnetite film when the unit is placed in operation after proper and complete cleaning. Over the passage of time, the protective film becomes overlaid with more porous magnetite scales, which consist of iron oxide corrosion products transported from the feed water system[6, 7]. Because of porosity, these scales have much lower heat transfer coefficient than the tube metal and can eventually reduce boiler efficiency and which may lead to localized overheating of tubes. These scales can also act as concentration sites for the potentially corrosive chemicals, which normally are at low concentrations in the bulk of boiler feed water. Most of the of iron oxide scales are usually generated during the boiler startups. Iron oxide usually constitutes the bulk of boiler tube scales and which necessitates periodic cleaning of the boiler components. One of the major operational issues with oxide deposition is that the particles precipitate predominately on the hot side of the tubes[8, 9]. At elevated temperatures, the potential for the under deposit corrosion mechanisms will proceed more rapidly on the hot side of the tubes[10, 11].

An efficient model based predictive methodology for scale deposition rate on the inner surface of waterwall tubes of coal fired boilers would be a valuable aid to the power plant engineers and boiler chemist which may provide guidelines to estimate remaining life of boiler tubes. In addition, it provides knowledgebase to envisage strategies to combat corrosion. For prediction of formation of scales and subsequent deposition on heat transfer surfaces of boiler assembly, it is imperative to have pertinent experimental data which will be required by the model to predict process behavior in a quantitative manner. The first principle based kinetic model necessitates critical information on kinetic rate parameters and transport process variables such as local flow velocity, local temperature of the water, temperature of heat transport surfaces, porosity and thermal conductivity of scales, uniformity of surface heating and time of contact of water with the surface. The deposition kinetics is also influenced by localized transport processes which are some times strongly coupled. These parameters needs to be estimated from controlled experiments which is fairly cumbersome. Quantitative determination of scale deposition rates in conjunction with pertinent mechanisms(such as flow assisted corrosion) as a function of water chemistry and operating parameters based on first principle kinetic modeling has remained a difficult subject. This is because of complex and probably non-linear relationship between the dependent and independent variables such as composition and quantity of scales, operating parameters and kinetic rate coefficients of scale deposition process. Therefore, first principle based kinetic model predictions are not always amenable to a realistic plant operating conditions. Therefore, often simplified assumptions are made to overcome phenomenological complexities. Of late, the Data driven Artificial Intelligence (AI) or Computational Intelligence (CI) based techniques are increasingly used successfully to functionally map the input-output relationship of complex chemical processes accurately. AI techniques (such as ANN, Fuzzy logy and Genetic algorithms), in principle, are intelligent information-treatment system with the characteristics of adaptive learning.

Application of an artificial neural network (ANN) model has been reported for data driven modelling and prediction of ash deposition in boiler heat transport system[12]. ANN has also been developed to successfully characterize thermal behavior of boiler tubes in the presence of fouling on the basis of plant data[13] and it has also been reported that such models have been applied to control and minimize the effect of fouling in biomass boilers[14]. Afghan et al.[15] provided a basic concept of an expert system for boiler fouling assessment theoretically. A comparative study of Fuzzy logic and ANN has been reported[16] for the prediction of remaining life of boiler tubes subjected to various damage mechanisms. Zhen et al.[17] attempted an adaptive Neuro-Fuzzy technique for forecasting coal slagging in a power plant. However, application of ANN modeling to predict the oxidation scale deposition rate in boiler operations is relatively scanty in the published literature.

The objective of the present work is to develop a multi-layer feed forward ANN model to predict explicitly the deposition rate of oxide scale as a function of measured plant data (input/output parameters), namely heat flux, pH, total dissolved solids, specific conductivity, iron concentration, silica concentration, phosphate content, sodium content and dissolved oxygen concentration of the feed water system of a typical coal fired Indian operating boiler. The proposed ANN model also attempts to characterize effects of some of

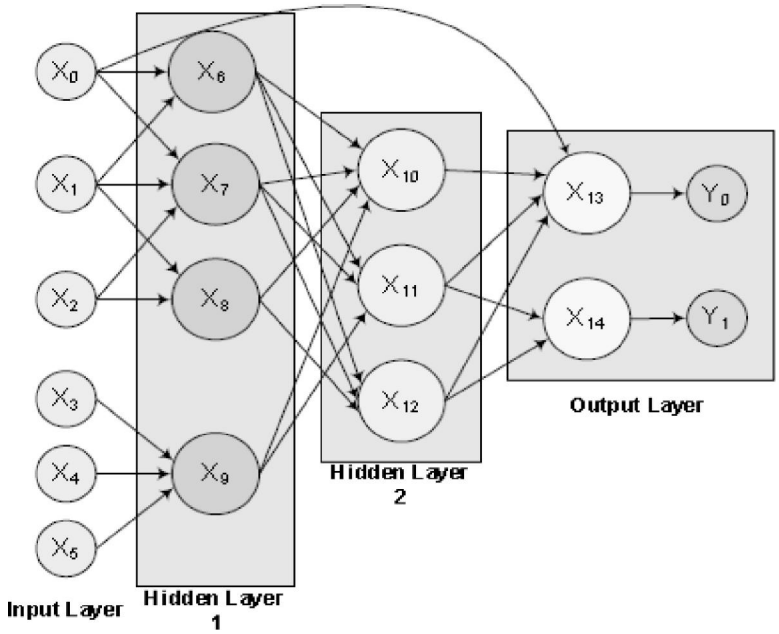

Figure 4 : Typical neural network architecture with input, hidden and output layers.

the operational parameters on the behavior of rate of scale deposition. In this proposed ANN model, Broyden-Fletcher-Goldfarb-Shanno (BFGS) network optimization algorithms with optimized neural network architecture have been incorporated to improve the network learning algorithm and to minimize the training error during the network learning process.

Measurement of plant data

Plants measurements have been carried out to generate the requisite data for neural network modeling. The salient features of the measurement are described below. Several samples have been collected at various interval and sampling points from the Indian operating plant and tested in the laboratory. The parametric measurements are enumerated below.

(i) Heat flux measurement

Measurements of heat flux have been carried out using portable heat flux meters which are inserted in different inspection zones. The heat flux instrument has been inserted closely to the surfaces such that composite contribution from both convective and radiative thermal transport from the flame front could be captured within tolerable error limit. The tubular type instruments known as flux-tubes have been used to minimize the variation in the thermal conductivity of scale because of ash and slag accumulation over the instrument. Measured boiler tube wall temperatures were used for the evaluation of the heat flux. The measuring tube is fitted with two thermocouples in holes of known radial spacings. The thermocouples are led away to the junction box where they are connected differentially to give a flux related electromotive force which is recorded by a digital instrument.

(ii) pH, specific conductivity and total dissolve solids (TDS) measurement

Feed water samples at appropriate interval have been collected and tested in the water analysis laboratory. These parameters have been measured by using a portable pH meter and specific conductivity-cum - TDS meter. This apparatus functions like a typical voltmeter which consists of a pair of electrodes connected to a system capable of measuring small voltages of the order of millivolts. It measures the voltage (electrical potential) generated by the boiler feed water sample under investigation and compares the same with the voltage of a known standard solution as the reference voltage. Subsequently, it uses the difference in voltage (potential difference) to calculate the difference in pH. For the conductivity measurement, the same two electrodes with an applied AC voltage are placed in the water sample. This creates a current dependent upon the conductive behavior of the sample. The measuring device registers this current and displays the value either as electrical conductivity or TDS (ppm). The electrical conductivity is measured and the TDS is calculated by

a built-in empirical formula from the conductivity inputs.

(iii) Iron content measurement

Iron content in the feed water has been estimated by the colorimetric analysis procedures using the 1, 10-Phenanthroline Method. The procedure uses ferrous iron reagent powder containing 1, 10-Phenanthroline as an indicator combined with a reducing agent to convert all but the most resistant forms of iron present in the sample to Fe^{+2}.

(iv) Phosphate and silica content measurement

Phosphate and silica contents in feed water have been determined by the colorimetric analysis using UV spectrophotometer. The method used for the measurements are, namely, ascorbic acid rapid liquid method and heteropoly blue rapid liquid method respectively.

(v) Sodium content measurement

Sodium in boiler feed water was estimated using a portable sodium analyzer (waltron 9033 sodium analyzer ^{R} - low range). This analyzer is based on advanced *multipoint control unit (MCU)* technology. Common measuring points in a boiler system for online sodium measurement includes make-up water, condensate, boiler feed water, saturated steam and main steam.

(vi) Dissolved oxygen measurement

Dissolved oxygen content in the feed water has been determined by portable dissolved oxygen analyzer (Portable Oxi-Meter Multi 3410 ^{R}). In order to conduct the dissolved oxygen test, it is imperative to use grab samples because analysis needs to be carried out immediately. This is essentially a field test which has been undertaken as a onsite measurement.

(vii) Oxide scale thickness measurement

The oxide scales have been measured using ultrasonic high frequency (20 MHz broadband) instrument in the laboratory. This instrument has built in software framework that is capable of detecting appropriate echoes and measuring the short time interval between the two echo-peaks that represent the steel/oxide and oxide/air boundaries reflections. A pre -calibrated value of ultrasonic velocity has been utilized to compute the thickness of the oxide scale using appropriate time, velocity and thickness relationships. Since the quantum of data measured is large enough for tabulation in

TABLE 1 : A typical segment of measured plant data

Heat flux (KW/m^2)	pH	Specific conductivity (µsem/cm)	TDS (ppm)	Silica content (ppm)	Fe content (ppbx10)	Dissolved Oxygen (ppb)	Na content (ppm)	Phosphate content (ppm)	Iron oxide deposition rate ($kg/m^2.secx10^{-8}$)
54.2	9.37	4	4	0.02	0.4	4	0.5	2	4.44
54.2	9.37	4.09	4.14	0.021	0.41	4.09	0.21	2.07	4.62
57.2	9.36	4.1	4.14	0.021	0.41	4.1	0.29	2.07	4.65
64.6	9.34	4.14	4.21	0.021	0.41	4.14	0.21	2.11	4.71
70.6	9.33	4.15	4.23	0.022	0.42	4.15	0.54	2.12	4.76
73.6	9.33	4.16	4.24	0.022	0.42	4.16	0.12	2.12	4.78
78.0	9.32	4.19	4.28	0.022	0.42	4.19	0.19	2.14	4.82
82.4	9.32	4.22	4.32	0.022	0.42	4.22	0.32	2.16	4.99
89.8	9.32	4.36	4.53	0.024	0.44	4.36	0.12	2.27	5.05
92.8	9.32	4.42	4.62	0.024	0.44	4.42	0.39	2.31	5.07
97.1	9.29	4.46	4.69	0.025	0.45	4.46	0.58	2.35	5.24
98.5	9.28	4.52	4.77	0.025	0.45	4.52	0.41	2.39	5.39
104.3	9.27	4.53	4.79	0.025	0.45	4.53	0.42	2.4	5.48
110.4	9.23	4.72	5.08	0.027	0.47	4.72	0.44	2.54	5.52
114.9	9.21	4.8	5.21	0.028	0.48	4.8	0.2	2.6	5.57
116.3	9.18	4.9	5.35	0.029	0.49	4.9	0.54	2.68	5.67
119.2	9.18	4.9	5.35	0.029	0.49	4.9	0.27	2.68	5.69
139.7	9.17	4.94	5.41	0.029	0.49	4.94	0.35	2.71	6.26

manuscript therefore, a typical segment of the measured data is shown in the TABLE 1. The total amount of data was collected during plant operating period ranging from 40,000 to 100,000 hours of boiler operation.

MULTI-LAYER PERCEPTION BASED ANN MODEL

The fundamental elements of the ANN methodology comprises of: (i) the functionality between input-output of neurons; (ii) the topological structure of the network; and (iii) the values of the connected weights and thresholds of neurons. The MLP based ANN architecture is shown in Figure 1. MLP is an interconnection of perceptrons in which data and calculations flow in a single direction, from the input data to the outputs. The number of layers in a ANN is the number of layers of perceptrons. The output from a given neuron is calculated by applying a transfer function to a weighted summation of its input to give an output, which can serve as input to other neurons.. Mathematically this can be given as:

$$\alpha_{jk} = f_k\left(\sum_{i=1}^{N_{k-1}} w_{ijk}\alpha_{i(k-1)} + \beta_{jk}\right) \quad (1)$$

where α_{jk} is neuron j's output from k's layer β_{jk} is the bias weight for neuron j in layer k. The model fitting parameters w_{ijk} are the connection weights and f_k's are activation functions.

For predictions, the most popular error function is the sum-of-squared errors, or one of its scaled versions. This is analogous to using the minimum least squares optimization criterion in linear regression. Like least squares, the sum-of-squared errors is calculated by looking at the squared difference between what the network predicts for each training pattern and the target value, or observed value, for that pattern. This is given as:

$$E = \frac{1}{2}\sum_{i=1}^{N}\sum_{j=1}^{C}(t_{ij} - \hat{t}_{ij})^2 \quad (2)$$

Where, N is the total number of training cases, C is equal to the number of network outputs, t_{ij} is the observed output for the i^{th} training case and the j^{th} network output, and $\hat{t}_{ij}$ is the network's prediction for that case. As the number of training patterns increases, the sum-of-squared error increases. As a result, it is often useful to use the root-mean-square (RMS) error instead of the un-scaled sum-of-squared errors. The RMS expression is given as:

$$E^{RMS} = \frac{\sum_{i=1}^{N}\sum_{j=1}^{C}(t_{ij} - \hat{t}_{ij})^2}{\sum_{i=1}^{N}\sum_{j=1}^{C}(t_{ij} - \bar{t})^2} \quad (3)$$

where $\bar{t}$ is the average output, given as :

$$\bar{t} = \frac{\sum_{i=1}^{N}\sum_{j=1}^{C} t_{ij}}{N.C} \quad (4)$$

Similar to E^{RMS}, a scaled version of the Laplacian error(L^{RMS}) can be calculated using the following formula:

$$L^{RMS} = \frac{\sum_{i=1}^{N}\sum_{j=1}^{C}|t_{ij} - \hat{t}_{ij}|}{\sum_{i=1}^{N}\sum_{j=1}^{C}|t_{ij} - \bar{t}|} \quad (5)$$

Gradient based network learning algorithm

Optimization of ANN's are concerned with the minimization of a particular objective function with respect to certain constraints. ANN's are proven highly efficient optimization tools. The objective of the network training is to find the optimal weights to minimize the errors between the prediction and the actual response. A popular criterion is the minimum-squares error between the prediction and the actual response. There are many different types of ANNs, differing by their network topology and/or learning algorithm. Back-propagation (BP) learning and network optimization algorithm, which is one of the most commonly used algorithms is designed to predict the output parameters.

Network training uses one of several possible optimization methods to minimize this error term. There are various BP algorithms such as Scaled Conjugate Gradient (SCG), Levenberg-Marquardt (LM), Gradient Descent with Momentum (GDM), variable learning rate Back propagation (GDA) and Resilient back Propagation (RP).[18]. There is variety of network optimization techniques that uses gradient of a function to be optimized. The general idea behind the so-called quasi-Newton optimization techniques is to build up an ap-

proximate expression for the Hessian matrix or the inverse Hessian, and use it to take an approximate Newton step. The most recently developed highly efficient version of the quasi-Newton optimization methods is the BFGS algorithm[19-21], which has largely replaced the classical Davidon-Fletcher- Powell (DFP) algorithm.

The Hessian matrix describes the local curvature of a function of many variables in an optimization problem. This Hessian matrix *H*[22-25] in general can be approximated as :

$$\mathbf{H} = \mathbf{J}^T\mathbf{J} \quad (6)$$

and the gradient can be computed as

$$\mathbf{g} = \mathbf{J}^T\mathbf{e} \quad (7)$$

Where, *J* is the Jacobian matrix which contains first derivatives of the network errors with respect to the weights. J^T is the transpose of matrix *J* and *e* is a vector of network errors. The *J* matrix can be computed through a standard back propagation technique that is less complex than computing the Hessian matrix.

In general, the quasi-Newton method was derived from quadratic objective function. The inverse of the Hessian matrix, H (shown in eqn. 6) is used to bias the gradient direction.

$$\mathbf{B} = \mathbf{H}^{-1} \quad (8)$$

In the quasi-Newton training method, the weights are updated using the following iterative procedure,

$$\mathbf{W}_{i+1} = \mathbf{W}_i - \eta\mathbf{B}_i\mathbf{g}_i \quad (9)$$

The matrix B here need not be computed. It is successively estimated employing rank 1 or rank 2 updates, following each line search in a sequence of search directions. This is algorithmically given as follows

$$\mathbf{B}_i = \mathbf{B}_i - \Delta\mathbf{B}_i \quad (10)$$

In this iterative algorithm, B_i*-1* is the previous value of *B*.

The two important algorithmic relationships to compute ΔB_i are as follows[24, 25]

$$\Delta\mathbf{B}_i = \frac{\mathbf{d}\mathbf{d}^T}{\mathbf{d}^T\Delta\mathbf{g}} - \frac{\mathbf{B}_{i-1}\Delta\mathbf{g}\Delta\mathbf{g}^T\mathbf{B}_{i-1}}{\Delta\mathbf{g}^T\mathbf{B}_{i-1}\Delta\mathbf{g}} \quad (11)$$

The above expression pertains to DFP algorithm. Alternatively, BFGS algorithm can be invoked using eqn.11

$$\Delta\mathbf{B}_i = (1 + \frac{\Delta\mathbf{g}^T\mathbf{B}_i - 1\Delta\mathbf{g}}{\mathbf{d}^T\Delta\mathbf{g}})\frac{\mathbf{d}\mathbf{d}^T}{\mathbf{d}^T\Delta\mathbf{g}} - \frac{\mathbf{d}\Delta\mathbf{g}^T\ \mathbf{B}_i - 1 + \mathbf{B}_i - 1\Delta\mathbf{g}\mathbf{d}^T}{\mathbf{d}^T\Delta\mathbf{g}} \quad (12)$$

Where,

$\mathbf{d} = \mathbf{w}_i - \mathbf{w}_{i-1}$ and $\Delta_g = \mathbf{g}_i - \mathbf{g}_{i-1}$, $\Delta\mathbf{B} = \mathbf{B}_i - \mathbf{B}_{i-1}$

The BFGS algorithm has the advantage over DFP in that it does not require accurate line minimizations along the quasi-Newton directions to build up the approximate Hessian matrix. Thus, BFGS potentially reduces the number of function evaluations required to achieve an optimization procedure.

IMPLEMENTATION OF THE ANN MODEL FOR BOILER OXIDE SCALE PREDICTION

Several chemical mechanisms contribute to the formation of oxide scale during operation of coal fired boiler. The limitation in acquisition of real time data during boiler operation and subsequent critical analysis is probably one of the major obstacles in building a database for data-driven modeling and online applications of AI based expert system in a plant.

Activation function for network training

The activation functions and its derivatives used in the present ANN model are shown in TABLE 2. In order to obtain the best network functionality, three optimal networks architecture has been generated. The nine numbers of input neurons representing the water chemistry and operating parameters (pH, specific conductivity, total dissolved solid, total iron concentration, silica concentration, phosphate concentration, sodium concentration, dissolved oxygen level of the feed water and heat flux) have been selected. One output neurons represent the scale deposition rate.

The activation function in the hidden layer was selected to be a sigmoid function:

$$\mathbf{f(x)} = \frac{1}{1+\exp(-\mathbf{x})} \quad (13)$$

An error back-propagation algorithm was adopted to learn the weights in the ANN

Network architecture and input-output variables

The input, output variables and their data ranges for a 250 MW typical Indian coal fired boiler system used in the ANN models are shown in TABLE 3. The operating temperature range and pressure ranges for feed water in the water walls for the desig-

TABLE 2 : Activation functions and its derivatives used in neural model

Activation Function	f(a)	$f'(a)$
Linear	$f(a)=a$	$f'(a)=1$
Logistic	$f(a)=\frac{1}{1+e^{-x}}$	$f'(a)=f(a)(1-f(a))$
Hyperbolic-tangent	$f(a)=\tanh(a)$	$f'(a)=\sec h^2(a)=1-\tanh^2(a)$
Squash	$f(a)=\frac{a}{1+\lvert a\rvert}$	$f'(a)=\frac{1}{(1+\lvert a\rvert)^2}=(1-\lvert f(a)\rvert)^2$

TABLE 3 : Operating data range of a typical Indian 250MW boiler for the ANN model

	Input Parameters	Data Range
1	Boiler feed water operating pH range	8.8-9.2
2	Specific conductivity (micro-seimens/cm)	3.0-8.0
3	Total dissolved solids (ppm)	5-10
4	Total iron concentration (ppb)	5-10
5	Silica concentration (ppm)	0.02-0.06
6	Phosphate concentration (ppm)	1.5-5.0
7	Sodium concentration (ppb)	5-10
8	Dissolved oxygen concentration (ppb)	5-10
9.	Heat flux operating range (KW/m^2)	50-300
	Output Parameter	
1.	Measured scale deposition rate (kg/m2.sec). 10^{-8}	4.10^{-8}-12.10^{-8}

nated boiler are 300-350C and 150-170 Kg/cm^2 respectively. Input data set is segmented into three subsets, namely, one for training (learning),one for selection (validation), and one for testing (prediction) using roughly 2:1:1 ratio. Out of 600 dataset from plant measurements, 300 dataset are used as training samples, 150 as validation samples and the remaining 150 samples have been utilized for prediction. The basis of selection of these three dataset for training, selection, and testing has been random. In order to obtain the optimum network, 20 networks are first designed with nine input neurons and one output neuron, four hidden layer is considered for the network. In total, twenty networks have been trained, out of which the best three network configurations have been chosen for prediction. The basic philosophy of MLP based network is that, too few neurons in the hidden layer may introduce higher error during network selection in the model, where the relations between different variables are not well developed. On the other hand, too many neurons in the hidden layer cause the model to over-fit the training data, resulting in a less optimal solution for selection data. The neural prediction based on three network architectures (MLP 9-4-1, MLP 9-6-1 and MLP 9-5-1) are compared with the regression fit between predicted and measured (test) oxide scale deposition rate data. It may be observed from the simulation results that all these three network architectures have almost similar accuracy level. Typically, the network architecture nomenclature, (say) MLP 9-4-1 specify a multi layer perceptron network and the subsequent digits indicate the number of input neurons(9), the number of hidden neurons(4) and number of output neurons(1) respectively

RESULT AND DISCUSSION

The present ANN simulation is based on the data measured from a typical Indian operating power plant. Figure 5 depicts neural prediction of oxide scale deposition rate on boiler water wall tubes made of carbon steel in an operating heat flux regime of 50-300 KW/m^2. The neural predictions are found to be in excellent agreement with the measured data. This establishes the

Full Paper

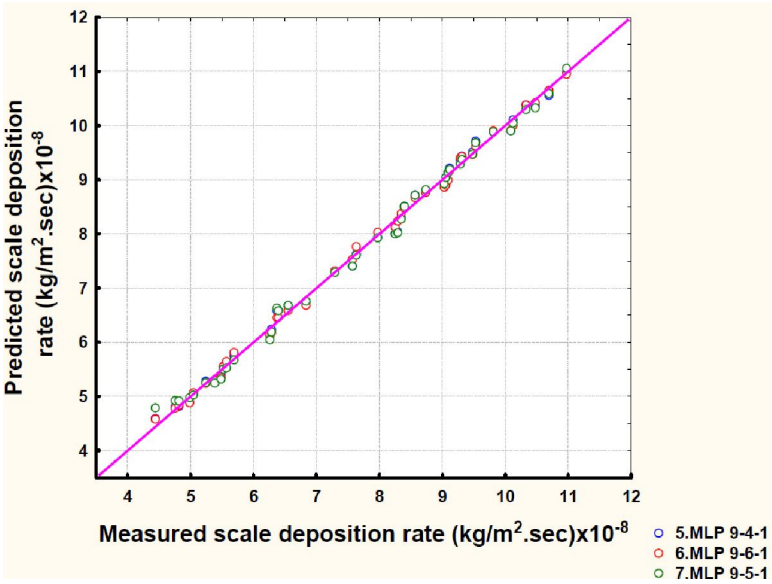

Figure 5 : ANN prediction and validation with the test data of oxide scale deposition rate on boiler tubes

efficient predictive capability of the ANN model in conjunction with the proposed optimal network architecture. Figure 6 shows predicted oxide scale deposition rate as a function of heat flux across the boiler tubes. It may be observed from the figure that the deposition rate monotonically increases with elevated heat flux. Further, these scale deposition rate varies from 4.6 x10^{-8} kg/m^2-sec to 11x10^{-8} kg/m^2-sec (appox) with respect to heat flux operating regime of 50 – 300 KW/m^2. This is attributed to the phenomenon that as the energy supplied in the form of heat increases, the number of nuclei formed also increases. All nuclei do not become scale particles, and able to reach the surface. Only those particles that have adequate energy and mass are able to reach the surface of the water walls and deposit on it. With an increase in heat flux the more proportion of particles making scale enhances. Figure 7 shows predicted oxide scale deposition rate as a function of pH of boiler feed water. It may be observed from the figure that the oxide scale deposition rate monotonically decreases with increased pH value (within the specified range) of the boiler feed water. The oxide scale deposition rate varies from 10.3 x10^{-8} kg/m^2-sec to 4.5 x10^{-8} kg/m^2-sec (appox) with respect to pH range of feed water, 8.8 -9.4. The predictions conform to the realistic operational conditions[22]. Maintaining a pH of 9 or greater reduces both the potential for ferrous alloy equipment failure and the return of iron corrosion products to the boiler feed water. In accordance with plant observation[23-26], too high pH (> 10) may initiate caustic gouging because gouging of boiler tubes has been commonly attributed to the dissolution of a protective magnetite film due to caustic attack, followed by precipitation of a non-protective magnetite scale. Figure 8 shows predicted oxide scale deposition rate as a function of total dissolved solids (TDS) in the boiler feed water. It may be observed from the figure that the scale deposition rate gets enhanced with increased value of TDS in feed water. The scale deposition rate varies from 4.8 x10^{-8} kg/m^2-sec to 10.7 x10^{-8} kg/m^2-sec (appox) with respect to TDS range of feed water i.e 4-10 ppm. High TDS water tends to foam which, when carried over by steam, leads to corrosion and depositition on heat transfer surfaces. Figure 9 shows predicted oxide scale deposition rate as a function of iron content present in the boiler feed water. It may be observed from the figure that the iron scale deposition rate enhances with increased value of iron content of boiler feed water which is consistent with the realistic observation[10, 22, 26, 27]. The oxide scale deposition rate varies from 4.9 x10^{-8} kg/m^2-sec to 10.6 x10^{-8} kg/m^2-sec (appox) with respect to total iron content of feed water in the range 0.4 - 0.8 ppm. When the increased concentration of iron corrosion products in boiler water exceeds iron solubility limit consequently leading to enhanced scale deposition. Figure 10 depicts variation of predicted scale deposition as a function of silica content of feed water. It may be observed from the figure

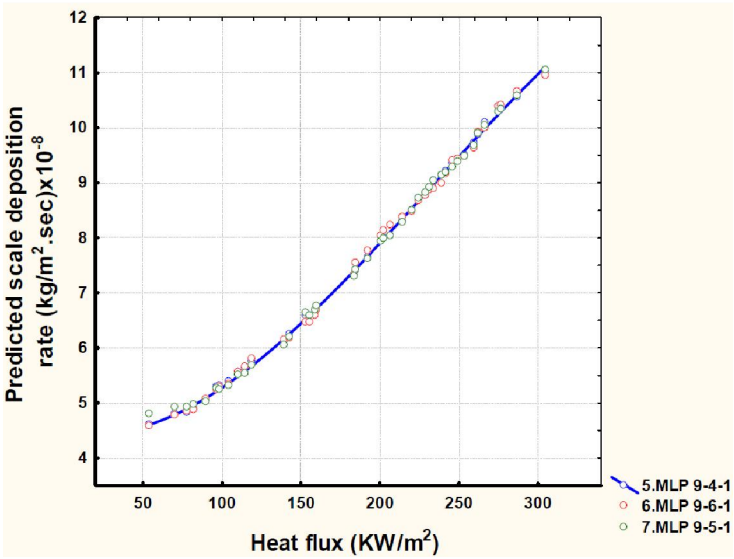

Figure 6 : Variation of predicted scale deposition as a function of heat flux on boiler tube

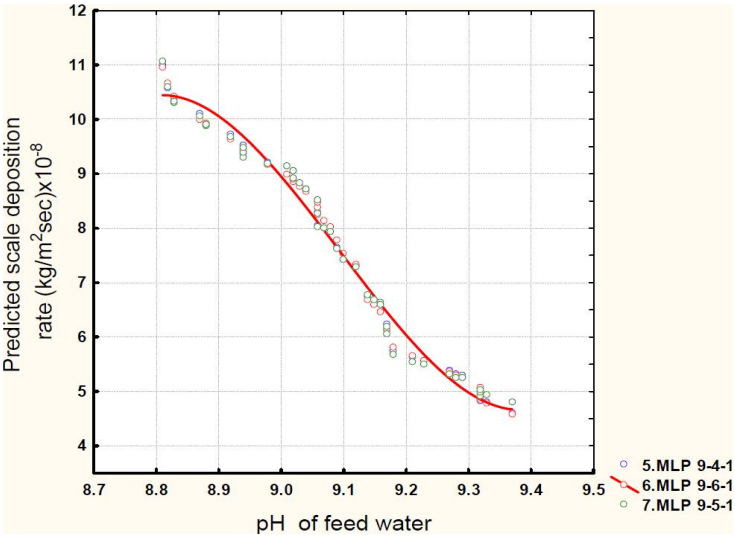

Figure 7 : Variation of predicted scale deposition as a function of pH of feed water

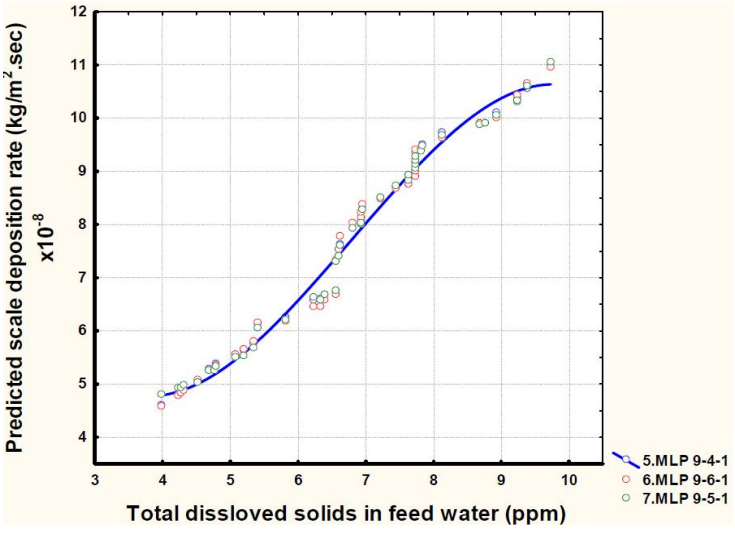

Figure 8 : Variation of predicted scale deposition as a function of total dissolved solid of feed water

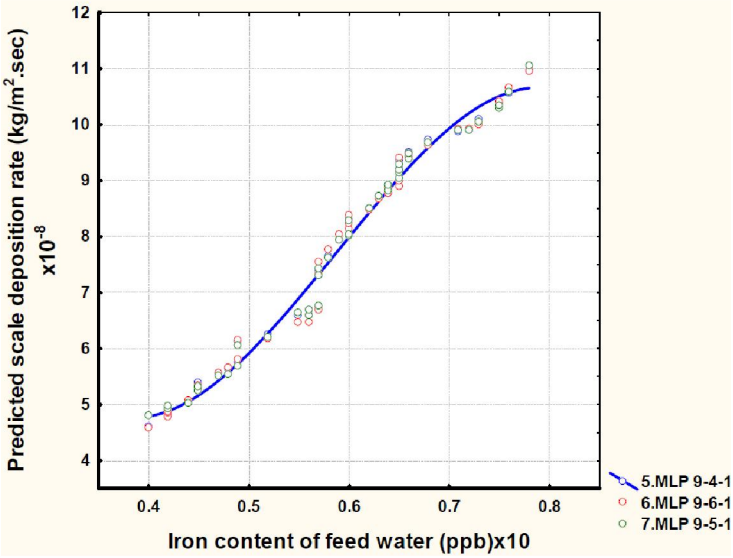

Figure 9 : Variation of predicted scale deposition as a function of Iron content of feed water

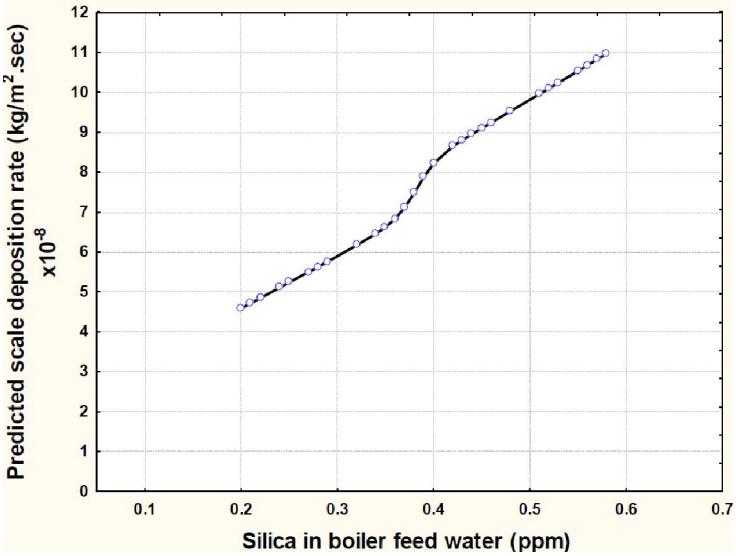

Figure 10 : Variation of predicted scale deposition as a function of silica content of feed water

that the total scale deposition rate enhances with increased value of silica content of boiler feed water. Higher concentration of silica generally precipitates directly on the boiler heat transfer surfaces and are much harder to remove from the boiler components. Figure 11 depicts variation of predicted scale deposition as a function of specific conductivity of feed water. It may be observed from the figure that the oxide scale deposition rate enhances with increased value of specific conductivity of boiler feed water. High specific conductivity of feed water is a consequence of high TDS in the same which incidentally leads to deposition of scales. Figure 12 depicts variation of predicted scale deposition as a function of dissolved oxygen content of feed water. It may be observed from the figure that the oxide scale deposition rate enhances with increased value of dissolved oxygen content of boiler feed water. High dissolved oxygen in the feed water results in the formation of increased iron corrosion product namely, hematite which eventually leads to deposition. The training and testing error evolution as a function of training cycles during ANN simulation is shown in Figure 13 It may be observed from this figure that the absolute error drops sharply from 0.06 to 0.01 at the very early stage of training (few cycles) and subsequently the training and testing errors asymptotically reduces to almost zero with further increase in the number of cycles. It may be further noted that the deviations in the measured data and

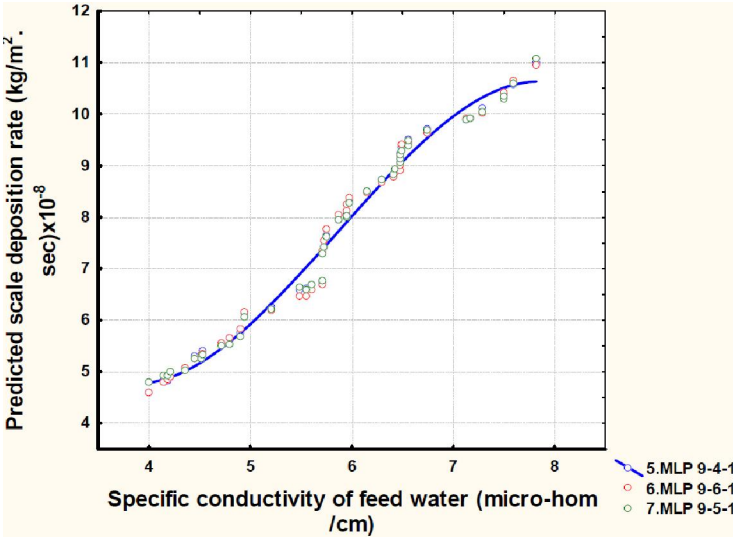

Figure 11 : Variation of predicted scale deposition as a function of specific conductivity of feed water

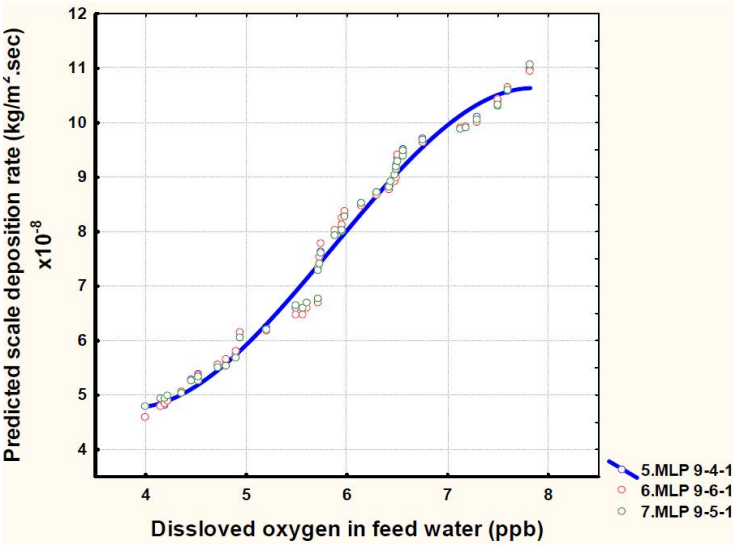

Figure 12 : Variation of predicted scale deposition as a function of dissolved oxygen in the feed water

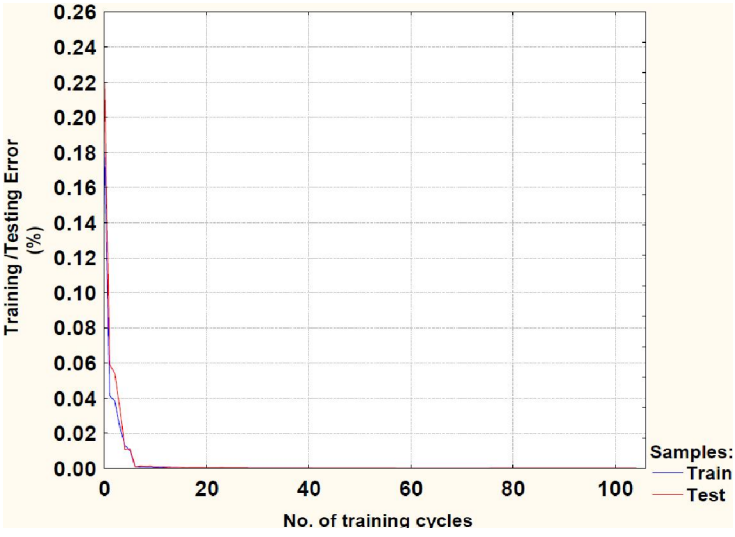

Figure 13 : Training and testing error convergence as a function of training cycles

neural predictions are substantially small. The present neural model with the selected architecture demonstrated accurate predictive capability of the model. There is scope of further improvement of the model by incorporating more process and operational parameter as inputs under realistic plant operating conditions.

CONCLUSION

This paper provides a brief ANN modeling framework for prediction of the oxide deposition rate on the water wall tubes of a coal fired boiler using plant generated data with good learning precision and generalization. Results of the neural network predictions are validated with those obtained from both plant and literature data. The main conclusions are as follows:

The proposed neural network model provides a reasonably accurate predictive framework and compare extremely well with the plant and experimental data. The ANN approach shows good potential for predictions of the deposition rate of oxide scale as a function of input variables, namely heat flux, pH, TDS, specific conductivity, iron concentration, silica content, phosphate content, sodium content and dissolved oxygen concentration of the feed water. This model has a relative advantage over other phenomenological and semi empirical models treating polluted data or the data with complex functional dependence. Effects of water chemistry and process parameters on the scale deposition behavior have been investigated. In the numerical domain, it has been found that BFGS is an effective optimization algorithm that does not require computation of numerically cumbersome Hessian matrix, or calculation of any matrix inverses. This algorithm potentially reduces the number of function evaluations required to achieve a network optimization facilitating faster convergence of training error within a few cycles.

REFERENCES

[1] N.N.Man'kina; Teploenergetika, **3**, 8 **(1960)**.
[2] M.I.Davidzon; Thermal Engineering, **55(7)**, 582 **(2008)**.
[3] J.Purbolaksono, A.Khinani, A.Z.Rashid, A.A.Ali, N.F.Nordin; Corrosion science, **51**, 1022 **(2009)**.
[4] J.Freeborn, D.Lewist; Journal mechanical engineering science, **l4**, 46 **(1962)**.
[5] B.M.Larin, E.N.Bushuev, E.V.Kozyulina, Yu.Tikhomirov; Thermal engineering, **52(10)**, 752 **(2005)**.
[6] N.N.Mankina, B.L.Lokotov; Teploenergetika, **9**, 15 **(1973)**.
[7] N.N.Mankina, M.M.Przhevalsky, Y.I.Blavatsky, I.N.Petrova; Teploenergetika, **2**, 79 **(1959)**.
[8] I.I.Chudnovskaya; Teploenergetika, **11**, 68 **(1979)**.
[9] D.Hasson, I.Perl; Desalination, **37**, 279 **(1981)**.
[10] V.P.Glebov; Teploenergetika, **3**, 55 **(1995)**.
[11] D.Hasso, M.Avriel, W.Resnick, T.Rozenman, S.Winderich; Ind.Eng.Chem.Fund, **7**, 59 **(1968)**.
[12] F.C.C.Lee, F.C.Lockwood; Progress in Energy and Combustion Science, **25**, 117 **(1998)**.
[13] Q.F.Yang, J.Ding, Z.Q.Shen; Chem.Eng.Sci, **55**, 797 **(2000)**.
[14] M.L.Thompson, M.A.Kramer; AIChE J, **40**, 1328 **(1994)**.
[15] N.H.Afgan, M.G.Carvalho, P.Coelho; Applied Thermal Engineering, **16**, 835 **(1996)**.
[16] A.Majidian, M.H.Saidi; International Journal of Fatigue, **29**, 489 **(2007)**.
[17] M.H.Dai; Int.J.Press Vessel Pip, **63**, 111 **(1995)**.
[18] G.Yagawa; Int.J.Press Vessel Pip, **63**, 303 **(1995)**.
[19] C.Trana, A.Abrahamb, L.Jaina; Neurocomputing, **6**, 185 **(2004)**.
[20] S.G.Nash, J.Nocedal, SIAM Journal of Optimization, **1**, 358 **(1991)**.
[21] Yuan, Ya-xiang; IMA Journal of Numerical Analysis, **11**, 325 **(1991)**.
[22] P.Boggs, J.Tolle; Acta Numerica, **4**, 11 **(1995)**.
[23] N.Gould, P.Toint; System modeling and optimization, methods, Theory and applications (Eds M.Powell and S.Scholtes, Netherlands Kluwer), 149 **(2000)**.
[24] S.K.Das; Ironmaking and Steelmaking, **40(4)**, 298 **(2013)**.
[25] I.Ghosh, S.K.Das, N.Chakraborty; Neural computing and application, Published Online 25th December, **(2013)**.
[26] T.I.Petrova, V.I.Kashinsky, A.G.Isianova, R.B.Dooley; Proceedings of 15th International Conference on the Properties of Water and Steam, Berlin, **(2008)**.
[27] M.J.Kalakodimi, G.E.Esmacher; Process and Water Technologies (Technical paper), 1 **(2009)**.